IOPscience iopscience.iop.org

Home Search Collections Journals About Contact us My IOPscience

Using the Gram-Charlier expansion to produce vibronic band shapes in strong coupling

This article has been downloaded from IOPscience. Please scroll down to see the full text article.

1992 J. Phys.: Condens. Matter 4 2347

(http://iopscience.iop.org/0953-8984/4/9/027)

View the table of contents for this issue, or go to the journal homepage for more

Download details:
IP Address: 171.66.16.159
The article was downloaded on 12/05/2010 at 11:27

Please note that terms and conditions apply.

J. Phys.: Condens. Matter 4 (1992) 2347–2359. Printed in the UK

Using the Gram–Charlier expansion to produce vibronic band shapes in strong coupling

M C M O'Brien

Oxford University, Department of Theoretical Physics, 1 Keble Road, Oxford OX1 3NP, UK

Received 9 October 1991, in final form 1 November 1991

Abstract. The Gram–Charlier expansion of a band is an expansion in Hermite polynomials multiplied by exponentials, which converges in the mean to the correct band shape, and its coefficients are linear combinations of moments of the band. It is shown here how this expansion can be used to simulate the vibronic band shapes resulting from various types of Jahn–Teller coupling. This process has the advantage of being at its best when the coupling is strong and the standard methods are difficult.

1. Introduction

This paper describes a novel way of calculating band shapes produced by strong coupling between electronic and vibrational degrees of freedom in a solid, and it aims to produce portraits of band shapes that are more valid than the result of Frank–Condon calculations in a regime where full quantum-mechanical calculations cannot be done. The interesting problems arise in particular when there is strong Jahn–Teller coupling between degenerate electron states and degenerate vibrational modes, the difficulty increasing with the degree of degeneracy on both sides. The background theory and a discussion of earlier work is to be found in a review article [1]. Briefly, the simple case of one electronic state interacting linearly with a single mode of vibration can be solved exactly at all coupling strengths to give a set of lines spaced at the phonon energy $\hbar\omega$, with intensities described by a Poisson distribution, which at strong coupling tends towards a normal (Gaussian) distribution. If our single electronic state is embedded in a solid, so that it can interact with many modes of vibration, then the band shape is just a convolution of the bands due to the different modes; the overall effect smooths out the line structure and the band shape tends to a smooth Gaussian at strong coupling. This Gaussian is the same as that predicted in the Frank–Condon approximation. In the more complicated Jahn–Teller case it is no longer possible to find an exact solution at any coupling strength, and instead a solution is usually found by a process of numerical diagonalization of the matrix of the Hamiltonian in a basis of the uncoupled electron states and phonon excitations. This process obviously gets less efficient as the coupling strength increases, but it has been used successfully at quite high coupling strengths in cases where the symmetry of the Hamiltonian can be used to cut down the size of the matrix. The results of such calculations can be compared with the predictions of the Frank–Condon approximation. It is found that

0953-8984/92/092347+13$04.50 © 1992 IOP Publishing Ltd

the convergence of the two is very much slower than in the simple case, and that families of resonances appear along the way. Some of these shapes have been successfully simulated [2–7], but there are still enough difficulties to make it highly desirable to devise another method of studying them.

In contrast to the previous method, which worked up from weak to strong coupling, we have here a method that works downwards and should be at its best when the coupling is very strong. It is based on the Gram–Charlier expansion [8], which is an expansion in Hermite polynomials multiplied by exponentials, and for which the coefficients are linear combinations of the moments of the band. These functions are well adapted to simulating localized functions such as band shapes or statistical distributions, as the exponential factor keeps them small outside a central region whose width can be chosen by the user. Used with care and in the right circumstances they can give a good representation of the band shape. From the point of view of the computation the use of moments is good, because they are simply produced by multiplication of the matrices, which are already at hand from previous band shape and other calculations. It is also favourable that the Hermite polynomials and their coefficients can be produced by recurrence relations that are computationally stable.

The question of assessment of the validity of the computed band shapes is an important one. We have approached it firstly by constructing bands whose shapes are already known, and secondly by changing the parameters to see which features of a band are stable, and therefore likely to be real. The first important thing is that this simulation is at its best when intensity changes across the band do not happen too sharply, and in particular it must not be asked to show any detail on the scale of the phonon structure, which is always smoothed out as one would expect in the strong coupling regime. It also gets into trouble if sudden changes in the intensity produce the wiggles associated with the 'Gibbs phenomenon' in Fourier analysis. These wiggles can be distinguished from genuine peaks by their position and lack of stability, but making this distinction may be quite difficult.

2. The Gram–Charlier expansion

The Gram–Charlier expansion is an expansion in orthogonal functions that converges in the mean to the function being represented. The formulae for the expansion can be written [8]

$$f(x) = \frac{1}{\sqrt{2\pi}} \exp\left(-\frac{1}{2}x^2\right)[c_0 + c_1 H_1(x) + c_2 H_2(x) + \cdots] \tag{1}$$

where $H_n(x)$ is the nth Hermite polynomial in x, defined by the recurrence relation

$$H_{n+1}(x) = xH_n(x) - nH_{n-1} \tag{2}$$

with $H_0(x) = 1$ and $H_1(x) = x$. The coefficients c_n are given by

$$c_n = \frac{1}{n!} \int_{-\infty}^{+\infty} H_n(x) f(x)\, \mathrm{d}x \tag{3}$$

and as $H_n(x)$ is just a polynomial of order n, so c_n is a linear combination of the moments of the distribution $f(x)$, including all the moments up to the nth. A choice

must be made of the scale and position of the origin for $f(x)$, and a sensible choice puts the origin at the centroid of $f(x)$, so that $c_1 = 0$, and sets the scale so that the second moment is 1, giving $c_2 = 0$. In this way the starting point is a Gaussian with the same centre and the same width as $f(x)$, which is clearly a useful start for an absorption band. In fact we make small changes in the scale and origin to suit different problems, but the approximation breaks down if we depart too far from this choice. The subsequent corrections in (1) are wavepacket-like functions, and figure 1 shows one of these.

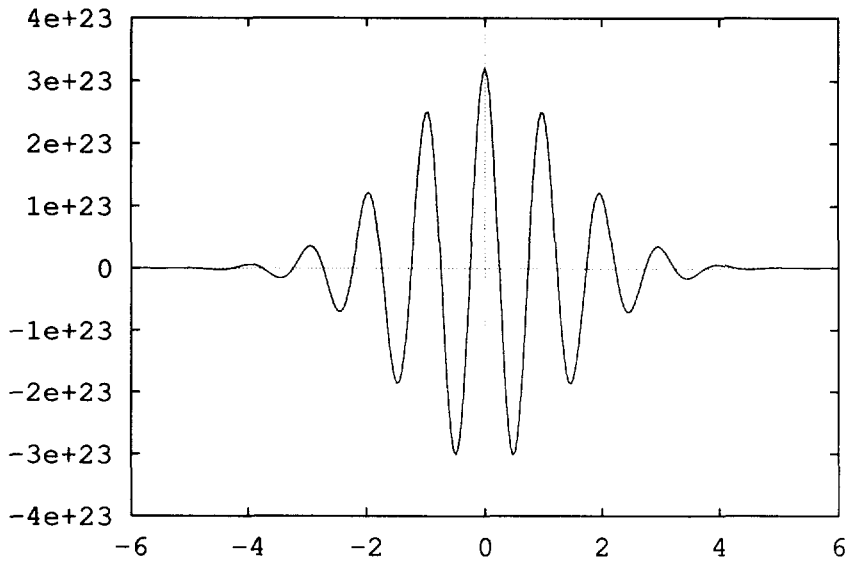

Figure 1. $H_{40}(x)\exp(-x^2/2)$.

2.1. The Gibbs phenomenon

This name is applied to the wiggles that appear in the sum of a Fourier series near a point where the function being synthesized has a sudden change of amplitude. These wiggles do not go away as the number of terms in the sum increases, they simply become taller and narrower in such a way that the square integral of the difference between the function and the sum goes properly to zero. Figure 2, which shows the result of performing a Gram–Charlier synthesis on a single delta function, illustrates this effect. The scale of the wiggles can be estimated by finding the wavelength in the 'wavepacket' functions, and for large n one can solve the appropriate differential equation in the WKB approximation, finding that the effective wavelength for $H_n(x)$ is $2\pi/\sqrt{n}$. This wavelength is the predicted distance between the real peak and the first subsiduary peak in the worst case. Clearly this represents a limit on the resolution of our method, though its effect can be reduced by a suitable choice of scaling.

3. Numerical methods

Any attempt to calculate either $H_n(x)$ or c_n, by adding and subtracting successive terms to the polynomial, soon runs into rounding errors because the terms are so much

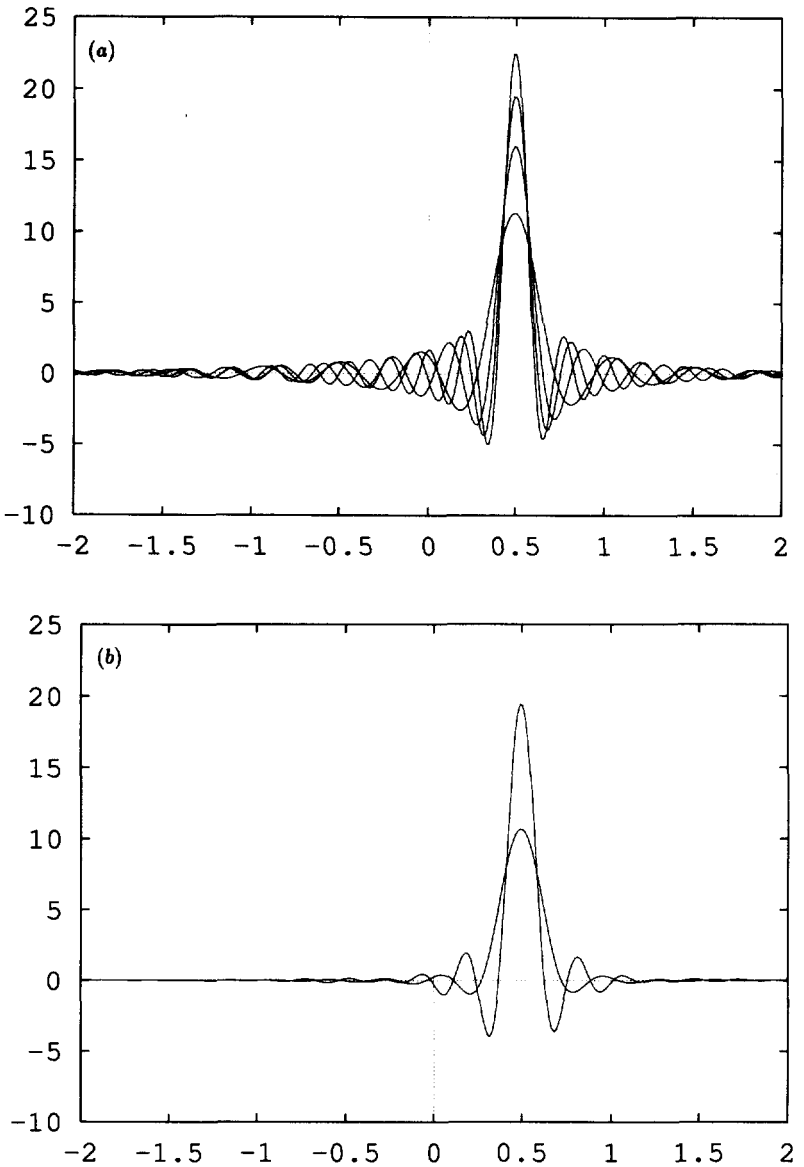

Figure 2. Simulation of a delta function (*a*) using 200, 400, 600 and 800 moments, (*b*) 400 and 800 moments with average over 400 terms.

larger than the final sum. That is why the recurrence relation (1) is so important. Its use to find values of $H_n(x)$ ensures that we have a reliable set of functions up to any value of n, and also that functions corresponding to only three successive values of n need to be kept at a time.

It is equally important to be able to compute the c_n using the recurrence relation, which is done in the following way. We start by setting up the matrix of the Jahn–Teller Hamiltonian in a basis of uncoupled electron and phonon states, with the uncoupled ground state in the $(1,1)$ position, so that in the absence of any coupling the allowed optical transition is to the first basis element only. Under those circumstances the nth

moment of the absorption band is given by

$$\mu_n = \langle 0 \mid A^n \mid 0 \rangle \tag{4}$$

where A is the matrix of the Hamiltonian and

$$|0\rangle = \begin{pmatrix} 1 \\ 0 \\ 0 \\ \vdots \end{pmatrix} . \tag{5}$$

(For a general discussion of the moments of a band see for example [9].) The matrix A is block tridiagonal, with no matrix elements connecting states that differ by more than 1 in their phonon occupation number. This means that if the bases for A stop at N phonons we can expect to be able to compute all moments up to μ_{2N}. Hermite polynomials in A can be constructed by the recurrence relation

$$H_{n+1}(A) = AH_n(A) - nH_{n-1}(A) \tag{6}$$

with $H_0(A) = [I]$, the unit matrix, and $H_1(A) = A$. Using (4) and (3) we accordingly find that

$$c_n = \langle 0 \mid H_n(A)/n! \mid 0 \rangle . \tag{7}$$

Although in principle this process requires matrix multiplication, in practice we can get away with only storing A and two basis vectors and using only a matrix × vector routine, as follows. We put $H_n(A)/n! \mid 0\rangle = \mid n\rangle$ and use (6) to give

$$|n+1\rangle = (A \mid n\rangle - \mid n-1\rangle)/(n+1) \tag{8}$$

and since $\langle 0 \mid n\rangle$ is just the first element of the vector $|n\rangle$ the coefficient c_n is immediately available. This numerical process works quite nicely, except for a difficulty with underflow. At large n, the c_n as defined here become too small and the $H_n(x)$ too large, but this can be cured by introducing a factor in the recursive definitions such that $c_n \rightarrow c_n \times (\text{FACTOR})^n$ and $H_n \rightarrow H_n/(\text{FACTOR})^n$, and choosing to have FACTOR $\sim$ 10–20 usually works.

An important choice that must be made is how to make the cut off in n. Since each extra term added in the series (1) reduces the integrated square difference between the function sought and the sum of the series, it appears that as many terms as possible should be included in full. However the behaviour of the Gibbs phenomenon makes the shape look better if we tail off the terms in some way. This is because of the behaviour that can be seen in figure 2—the wavelength of the wiggles varies with the value of n at cut off, so averaging over different values of n smooths out all but the dip nearest to the delta function, as can be seen in figure 2(b). That last dip inevitably remains, and just has to be discounted when looking at the shapes. Another example of the effect of averaging can be seen in figures 5(a) and (b). In practice it is also a good idea to calculate the same band shape with various values of the scale and the choice of origin so as to sort out computational artifacts. The choice of scale can also have a considerable influence on the speed of convergence as well as on the speed with which instability is reached.

The matrices A are very sparse, so storage only needs to be found for the non-zero elements. Even so, the limit on some of the computations described here was storage. In some cases this can be got round by recalculating the necessary matrix elements for each call of the routine for $A \times |n\rangle$. This loses some time but the loss is not always very great. In most of the cases discussed in the following sections, the matrix A has already been found and used for other calculations, so that it is relatively straightforward to take them over for this one, but details will be given case by case.

4. Jahn–Teller band shapes

4.1. $E \otimes \epsilon$

As always we start with this system, which is the simplest one that is also interesting. It will serve to show what good results can be obtained with this method. As is well known the Frank–Condon shape is a double hump, corresponding to the two adiabatic sheets, and the band shape shows this double-humped structure at quite weak coupling, but as the coupling strength increases resonances appear on the high energy end and gradually close up to recreate the double hump. These were calculated originally by matrix diagonalization [10], and figure 3 shows a recalculation of the band shape by the methods of this paper, using the same parameters. The number of moments used in each case was sufficient to converge well to the band shape, except for a slight wiggle at the centre of each band. The agreement with [10] is very close.

In this case the matrix A is tridiagonal, with only one base per phonon occupation number, so there were no particular difficulties of size or time in the computation. The size of the matrix goes as N where μ_N is the highest moment used, so very high values of N can be used.

4.2. $\Gamma_8 \otimes (\tau_2 \oplus \epsilon)$

This is another system that can be set up in a tridiagonal matrix [11], and in the 1977 paper some band shapes were shown, but these have not been repeated by later methods, so a sample is included here (figure 4). It should be noted that the dip in the middle of this band is deeper than in $E \otimes \epsilon$, so the numerical process generates a wiggle there. The resonances on the high-energy side of the band are correctly placed.

4.3. $T \otimes (\tau_2 \oplus \epsilon)$

This is the case of a p state in equal coupling with modes of the two different symmetry types, with spin–orbit coupling to a spin of $\frac{1}{2}$. The fact that the phonon states can be classified by their five-dimensional SO(5) symmetry helps to limit the size of the matrix, which goes as N^2, so that well-resolved band shapes have been found by matrix diagonalization [4]. None the less, experiments suggest that we should be looking at stronger coupling than can be achieved by matrix diagonalization [5], and we have accordingly produced some more band shapes with much stronger coupling by this new method (figure 5). The very strong coupling used here is shown by the large number of resonances showing up on the high-energy band. All three bands in figure 5 show the resonances on the peak at highest energy as well as the wiggles produced by the numerical process. Figures 5(a) and 5(b) have both been put in to show how the wiggles can be calmed down by averaging, at the expense of some loss in resolution. The origin of the resonances is discussed in [6].

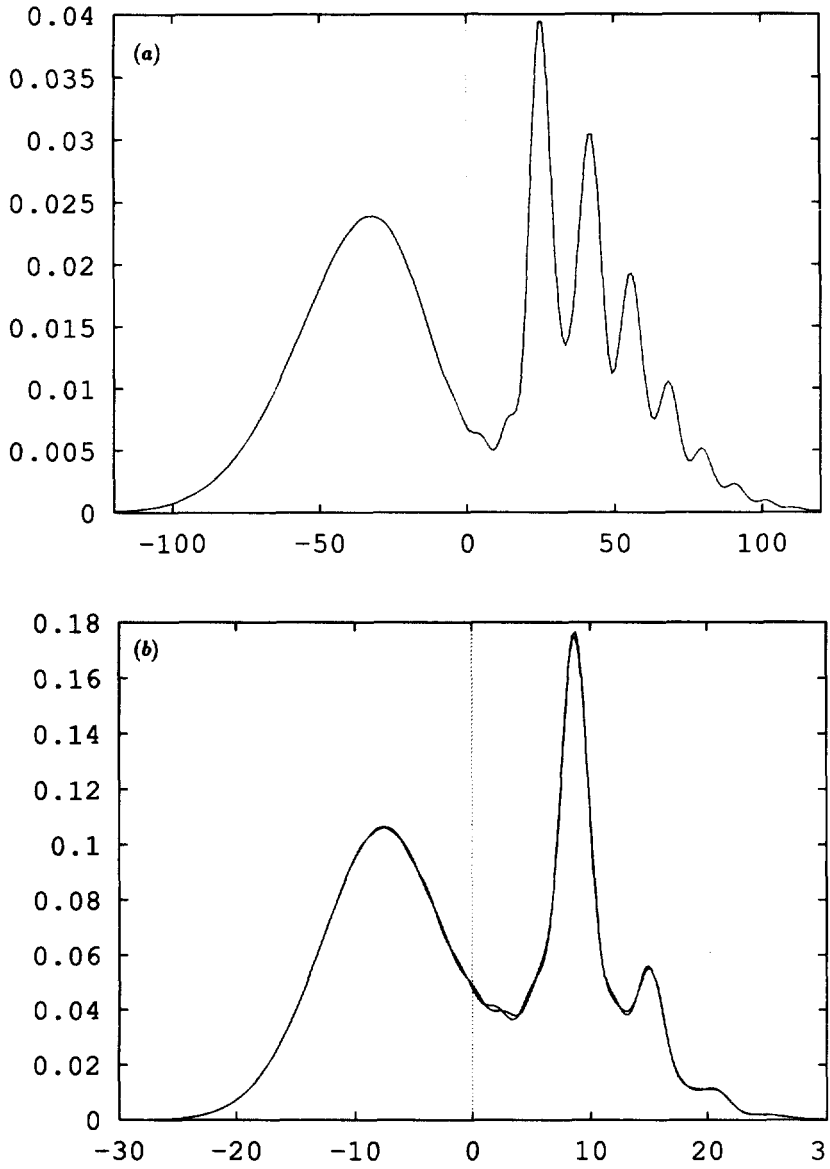

Figure 3. Band shapes for $E \otimes \epsilon$, coupling strengths as in [10], horizontal scale in units of $\hbar\omega$ here and elsewhere. (*a*) 1200 moments, (*b*) 600 moments.

Before leaving this system we include another pair of band shapes (figure 6) which compares the shape from (*a*) $\Gamma_8 \otimes (\tau_2 \oplus \epsilon)$ with that from (*b*) $T \otimes (\tau_2 \oplus \epsilon)$ when the coupling strength is the same, and the spin–orbit coupling is large enough to make a good gap between the $j = \frac{1}{2}$ and $j = \frac{3}{2}$ bands. These are plotted on the same horizontal scale, and with the origins matched. They are very similar, and the difference between them must be attributed to the coupling in (*b*) to the $j = \frac{1}{2}$ states not so far away. This comparison throws some light on the attempt in [11] to fit some experimental band shapes using $\Gamma_8 \otimes (\tau_2 \oplus \epsilon)$ theory. The general fit was good, but the balance between the strengths of the two peaks was wrong. Figure 6 suggests that

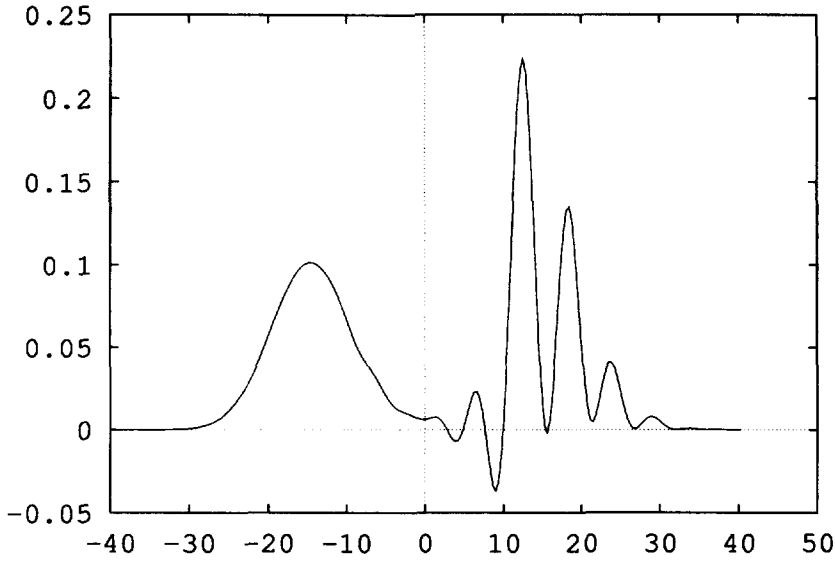

Figure 4. $\Gamma_8 \otimes (\tau_2 \oplus \epsilon)$ at 400 moments with $L = 10$. (L is the coupling strength defined in [11].)

we might have done better with $T \otimes (\tau_2 \oplus \epsilon)$.

4.4. $T \otimes \tau_2$

This system, an electronic p state coupled to τ_2-type normal modes, is the one that has been most intractable to numerical methods although it was studied early on. The difficulty arises because, unlike all those listed so far, it has no accidental symmetry higher than the intrinsic octahedral symmetry of the complex. This means that group theory cannot be used to thin down the basis states of the matrix very much, and computations have to be stopped because of their excessive size. The large size of the matrices also makes difficulties for the method used here, but the figures (7) and (8) show a great improvement on those produced previously. In 1966, Toyozawa and Inoue [12], in an elegant piece of analysis, showed that the semi-classical band shape had three peaks, with the central one being a logarithmic singularity, and figure 7(a) shows the approach to this shape at strong coupling. For comparison 7(b) shows the smoother three-peaked band shape for $T \otimes (\tau_2 \oplus \epsilon)$ at strong coupling.

It is also of interest to look at the band shapes with spin–orbit coupling, of which samples are shown in figure 8. These shapes are worth looking at because they could be used to try to match the experimental bands arising from s $\rightarrow$ p transitions mentioned in 4.3. All fittings of band shapes done so far have been based on the equal coupling model of 4.3 simply because this was the only way of getting tractable computations, and other models should be tried. In fact the figures show that with spin–orbit coupling it would be hard to distinguish shapes calculated from the two models; it is only when the spin–orbit coupling gets very small that the characteristic logarithmic singularity appears.

In this system two different methods were adopted to set up the matrices. In an effort to make the matrices as small as possible, the matrix derived using pseudoscalar operators [13] was used first, as it had been to do some preliminary calculations by

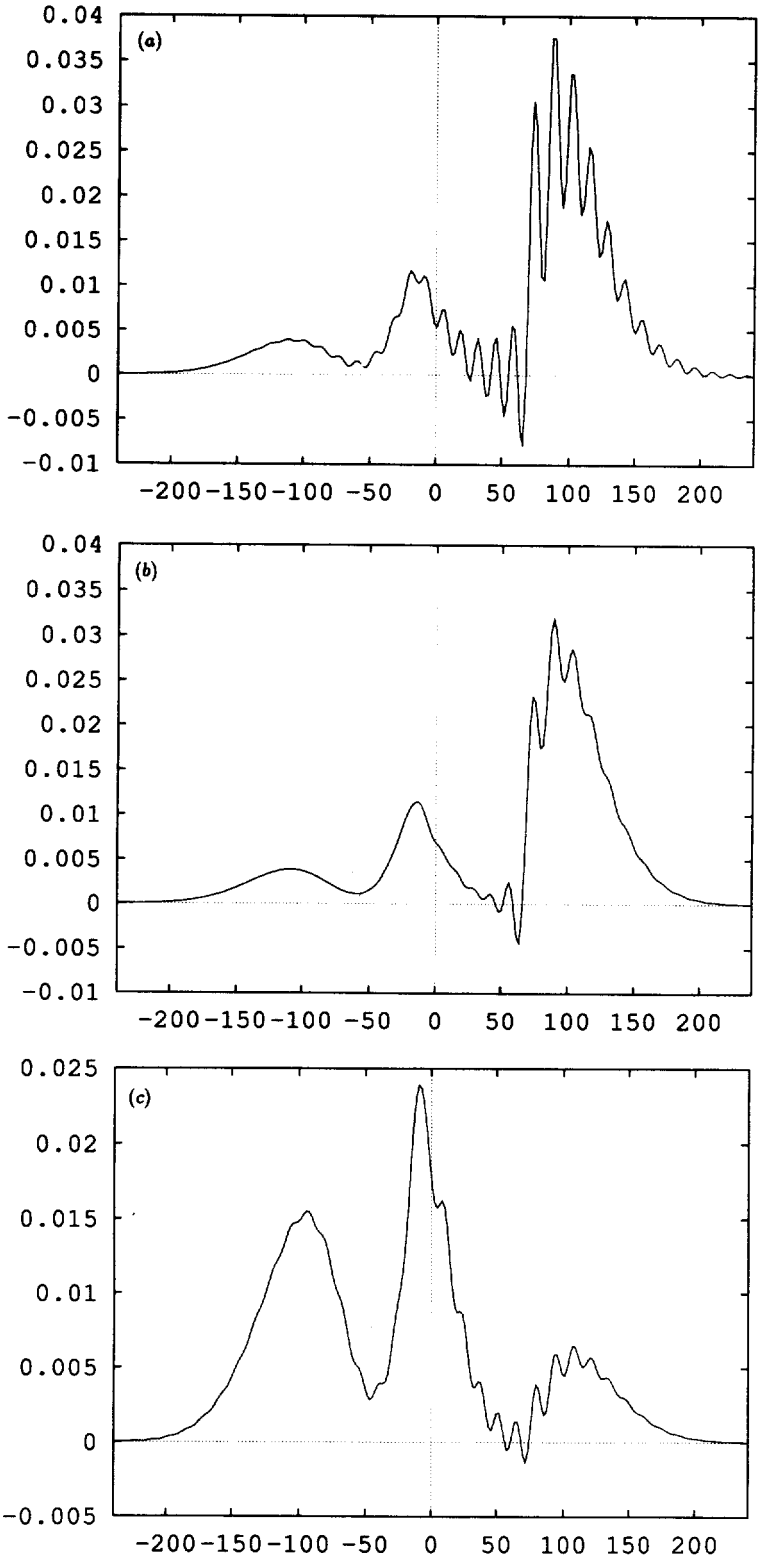

Figure 5. Band shapes for $T \otimes (\tau_2 \oplus \epsilon)$ with $k = 145$ and $\lambda = -0.4k$. (*a*), (*b*) $j = \frac{1}{2}$, 800 moments, but with (*b*) averaged over 400 moments; (*c*) $j = \frac{3}{2}$, 800 moments with averaging over 100.

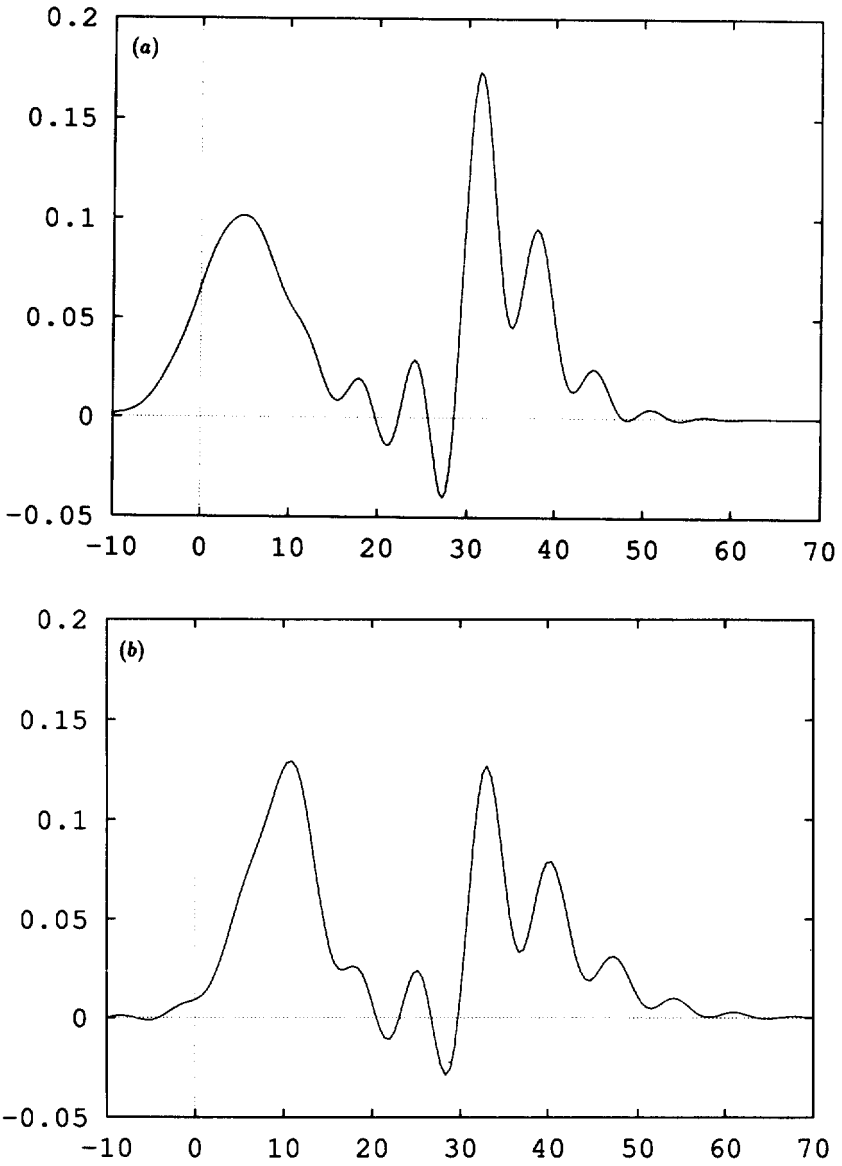

Figure 6. Band shapes for $j = \frac{3}{2}$ in equal coupling produced in two different ways (*a*) as $\Gamma_8 \otimes (\tau_2 \oplus \epsilon)$ and (*b*) as $\mathrm{T} \otimes (\tau_2 \oplus \epsilon)$ with spin–orbit coupling. Both used 240 moments. As usual the wiggles at the band centre are a result of the numerical process.

Kimber [7]. However it is complicated to set up, and would be even more complicated with the inclusion of spin–orbit coupling [14], so for most of this band-shape work the method of Sakamoto [15, 16] was used. This latter method uses larger matrices, but the simplicity of setting them up gives it a great advantage. In each case the size of the matrix goes as N^3, so this is the case for which the size and time limitation on the process is most severe, and is why we have not looked for high resolution in $\mathrm{T} \otimes \tau_2$.

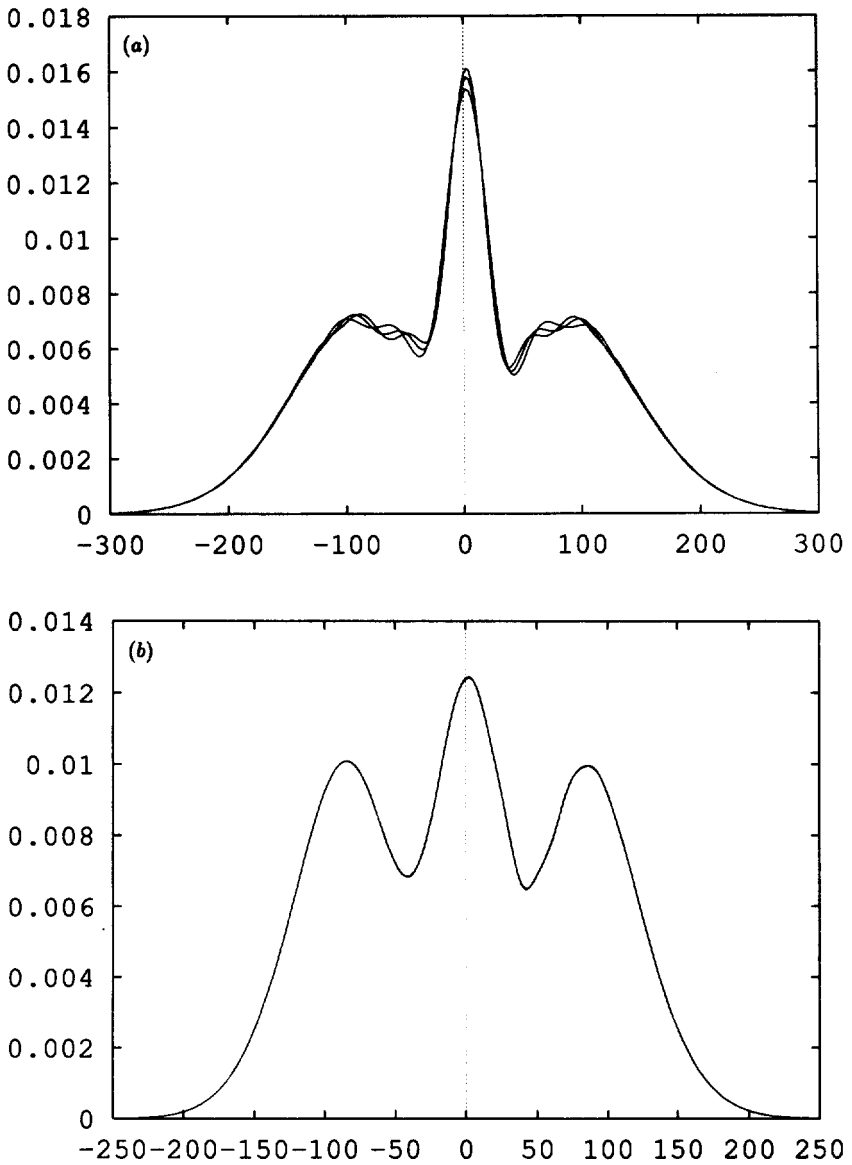

Figure 7. Band shapes for triplet states with no spin–orbit coupling. (*a*) $T \otimes \tau_2$, $k = 100$, shapes for 80, 100 and 120 moments; the wiggles on the outer peaks are produced by the sharpness of the central singularity. (*b*) $T \otimes (\tau_2 \oplus \epsilon)$ with $k = 145$ and 800 moments.

5. Conclusions

We have here a method for simulating vibronic band shapes in strong coupling that can give results where other methods fail because of the size of the matrices. The appearance of the Gibbs phenomenon makes the method a little trickier to use when the band intensity has very sharp changes, but averaging can help, and comparing results obtained with different scalings helps to distinguish between real and induced structure.

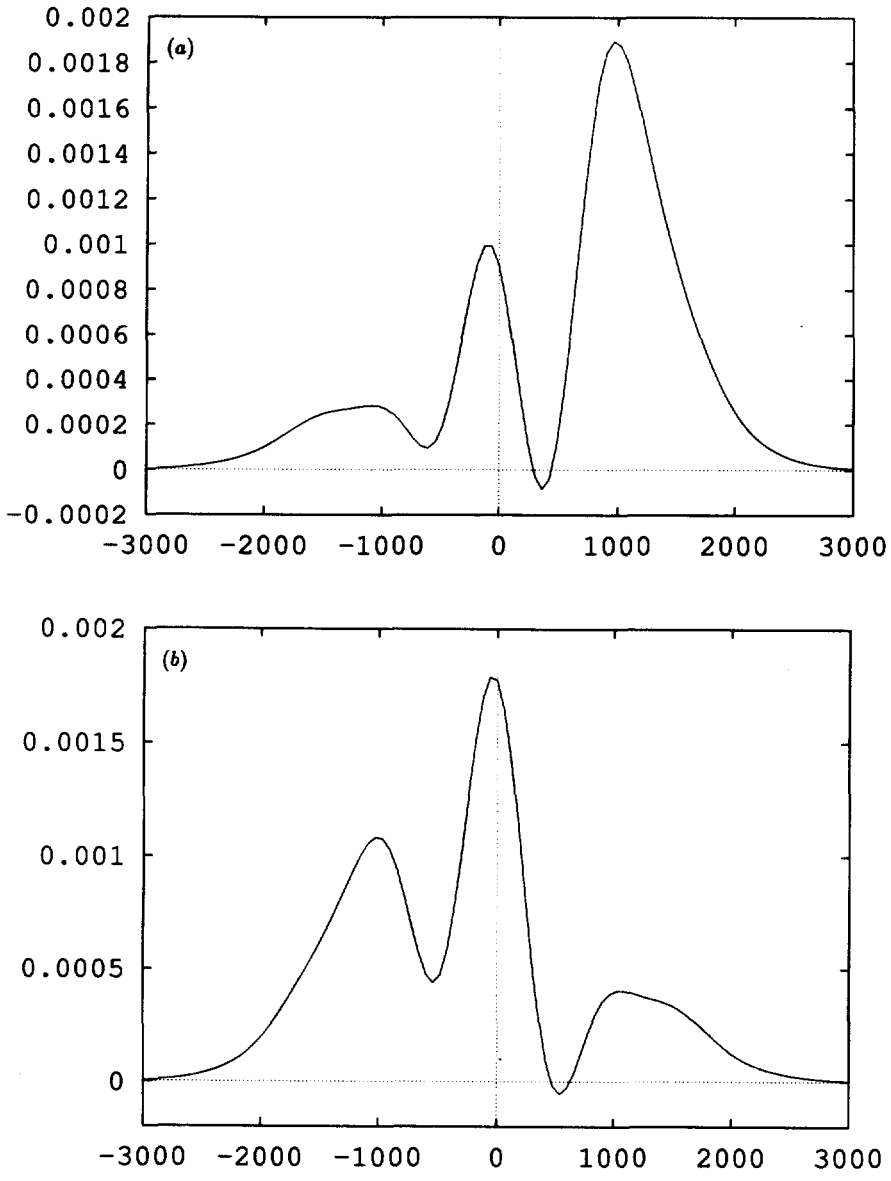

Figure 8. Band shapes for triplet states with spin–orbit coupling in $T \otimes \tau_2$; shapes for $k = 1000$, $\lambda = -0.3k$, 20 moments. (*a*) $\frac{1}{2}$ (*b*) $j = \frac{3}{2}$.

In a real solid other interactions frequently smooth over any sharp structures, and in this case it is shapes like those of figure 8, produced with rather few moments, that are needed to compare with experiment rather than shapes like that of figure 4. If the sharp spectra corresponding to many phonon excitations are used it must be recognized that these phonon excitations are only providing a basis set in which to do the calculations, whereas the Jahn–Teller coupling is providing a force that is much stronger than the normal elastic restoring forces, so the use of high phonon excitations does not necessarily imply anharmonicity in the forces.

Acknowledgments

I should like to thank the SERC for their provision of computing facilities, which were crucial for the work reported here.

References

[1] O'Brien M C M 1981 Vibronic Spectra and Structure Associated with Jahn–Teller Interactions in the Solid State *Vibrational Spectra and Structure* ed J R Durig (Amsterdam: Elsevier)
[2] Darlison A G 1987 *J. Phys. C: Solid State Phys.* **20** 5051–71
[3] O'Brien M C M 1985 *J. Chem. Phys.* **82** 3870–71
[4] O'Brien M C M 1985 *J. Phys. C: Solid State Phys.* **18** 4963–73
[5] Rose J, Smith D, Williamson B E, Schatz P N and O'Brien M C M 1986 *J. Phys. Chem.* **90** 2608–15
[6] Chancey C C and O'Brien M C M 1989 *J. Phys.: Condens. Matter* **1** 47–68
[7] Kimber A 1990 *D Phil Thesis* Oxford University
[8] Kendall M G and Stuart A 1969 *The Advanced Theory of Statistics* 3rd edn (Griffin)
[9] Henry C H and Slichter C P 1986 *Moments and Degeneracy in Optical Spectra* ed W Beall Fowler *Physics of Color Centers* (New York: Academic)
[10] O'Brien M C M and Evangelou S N 1980 *Solid State Commun.* **36** 29–32
[11] Pooler D R and O'Brien M C M 1977 *J. Phys. C: Solid State Phys.* **10** 3769–91
[12] Toyozawa Y and Inoue M 1966 *J. Phys. Soc. Japan* **21** 1663
[13] Borner H P and O'Brien M C M 1988 *J. Phys. A: Math. Gen.* **21** 4289–4304
[14] Borner H P 1986 *MSc Thesis* Oxford University
[15] Sakamoto N 1980 *J. Phys.: Condens. Matter* **48** 527–43
[16] O'Brien M C M 1990 *J. Phys.: Condens. Matter* **2** 5539–53